Journal of Magnetics 13(4), 124-127 (2008)

A First-principles Study on Magnetic and Electronic Properties of Ni Impurity in bcc Fe

Gul Rahman and In Gee Kim*

Graduate Institute of Ferrous Technology, Pohang University of Science and Technology, Pohang 790-784, Korea

(Received 27 October 2008, Received in final form 21 November 2008, Accepted 25 November 2008)

The magnetic and electronic properties of Ni impurity in bcc Fe (Ni_1Fe_{26}) are investigated using the full potential linearized augmented plane wave (FLAPW) method based the generalized gradient approximation (GGA). We found that the Ni impurity in bcc Fe increases both the lattice constant and the magnetic moment of bcc Fe. The calculated equilibrium lattice constant of Ni_1Fe_{26} in the ferromagnetic state was 2.84 Å, which is slightly larger than that of bcc Fe (2.83 Å). The averaged magnetic moment per atom of Ni_1Fe_{26} unit cell was calculated to be 2.24 μ_B, which is greater than that of bcc Fe (2.17 μ_B). The enhancement of magnetic moment of Ni_1Fe_{26} is mainly contributed by the nearest neighbor Fe atom of Ni, *i.e.,* Fe1, and this can be explained by the spin flip of Fe1 *d* states. The density of states shows that Ni impurity forms a virtual bound state (VBS), which is contributed by Ni $e_{g\downarrow}$ states. We suggest that the VBS caused by the Ni impurity is responsible for the spin flip of Fe1 *d* states.

Keywords : first-principles, magnetism, electronic structure, impurity, Fe, Ni

1. Introduction

Nickel and iron forms substantial solid solutions over the complete range of compositions. According to equilibrium phase diagram by Owen and Liu [1], the alloys at the temperature higher than 200 °C are in face-centered cubic (fcc) γ phase from pure Ni to ~70% Ni. The body-centered cubic (bcc) α phase is stable from pure iron to ~10% Ni. In the concentration range of 10~70% Ni there is a mixed phase ($\alpha + \gamma$) region. Increasing the Ni concentration in α-Fe stabilizes γ-Fe and Ni is commonly known as a γ-stabilizer [1]. Fe-Ni alloys are also of interest in connection with Invar effect and martensitic transformation from austenite to martensite phase at low temperatures and these issues are well addressed in the literature [2, 3]. In bulk phase, Fe-Ni alloys are among the most widely studied magnetic materials and Fe-Ni systems are very important for understanding the mechanical and magnetic properties of steels because the addition of nickel to iron greatly enhances the strength and corrosion resistance of steel.

Much attention has been given in the past to Fe-Ni alloys near Invar compositions or ordered compounds (Fe_3Ni, FeNi, or $FeNi_3$), but not to Fe-Ni alloys with Ni compositions less than 10% [2-5]. To further elucidate the effect of Ni impurity on lattice parameters, nearest neighbor interactions, magnetic moments, and electronic properties, we study the magnetic and electronic properties of Ni in bcc Fe using a first-principles calculation.

2. Computational Method

A 3 × 3 × 3 supercell of bcc Fe, which corresponds to 27 Fe atoms in the unit cell, was considered with Ni substitution of the body-centered Fe atom of the supercell; we denote the model as Ni_1Fe_{26}. This Ni concentration corresponds to 3.7 at.% of Ni in bcc Fe. In such cubic unit cell, Ni has three nearest neighbors, *i.e.*, Fe1, Fe2, and Fe3 are the 1st, 2nd, and 3rd nearest neighbors, respectively. The optimized lattice constant of Ni_1Fe_{26} was calculated by total energy minimization.

The Kohn-Sham equation was solved self-consistently by using the total energy all-electron full-potential linearized augmented plane-wave (FLAPW) method [6, 7] based on the generalized gradient approximation (GGA) [8] for the exchange-correlation potential. The FLAPW method has successfully applied to various systems includ-

*Corresponding author: Tel: +82-54-279-4409
Fax: +82-54-279-4499, e-mail: igkim@postech.ac.kr

ing surfaces, alloys, and interfaces [9-11]. The integrations over the three dimensional Brillouin zone (3D-BZ) were performed by the improved tetrahedron method [12] over a 13 × 13 × 13 Monkhorst-Pack mesh [13] in the 3D-BZ, which corresponds to 84 k-points inside the irreducible wedge of 3D-BZ. The linearized augmented plane wave (LAPW) basis set was expanded using a plane wave cutoff of 16 Ry. Lattice harmonics with $l \leq 8$ were employed to expand the charge density, potential, and wave functions inside each muffin-tin (MT) sphere. The MT radius of 2.20 a.u. was used for both Fe and Ni atoms. The star-function cutoff of 260 Ry was employed for depicting the charge density and potential in the interstitial region. The core electrons were treated fully relativistically, and the valence electrons were treated scalar relativistically. Self-consistency was assumed when the difference between input and output charge (spin) density was less than 1.0×10^{-5} electrons/a.u.^{3}

3. Results and Discussion

In Fig. 1, the total energy versus volume curves of (a) bcc Fe, (b) bcc and fcc Ni, and (c) Ni_1Fe_{26} of the paramagnetic (PM) and ferromagnetic (FM) states are presented. The circles and squares represent bcc and fcc structures, respectively. The filled and open symbols denote the FM and PM states, respectively. From these curves we obtained the equilibrium volumes (lattice constants) using the Birch-Murnaghan equation of state (EOS) [14] and the calculated lattice parameters are summarized in Table 1. We see the lattice constant of bcc Fe was found to be 2.83 Å (2.76 Å) in the FM (PM) state, which is comparable with the previous calculations of 2.84 Å in FM state and 2.76 Å in PM state [15, 16] and the experimental observations of 2.87 Å [17]. The calculated equilibrium lattice constant of Ni_1Fe_{26} was determined to be 2.84 Å (2.76 Å) in the FM (PM) state. In other words, the inclusion of Ni in bcc Fe expands the lattice constant of bcc Fe in the FM state, but not in the PM state. The increment of the lattice constant due to the Ni impurity in bcc Fe is consistent with the experimental observation [18], where it has been found that Ni impurities slightly expand the lattice constant of bcc Fe. The slight increase of lattice constant due to Ni is explained in terms of protuberances in the literature. For bcc Fe, the protuberances would not lie on the lines joining adjacent atom-centers, and the parameters of the space-lattice would be the same as if the protuberances did not exist. However, the substitution of a Ni atom for any of the Fe atoms must cause the protuberances to some or all of its neighbors and thus distend the space-lattice [18].

Table 1 also shows the calculated magnetic moments in units of μ_B of bcc Fe, bcc Ni, and fcc Ni as well as Ni_1Fe_{26}. In general, these results are found to be in good

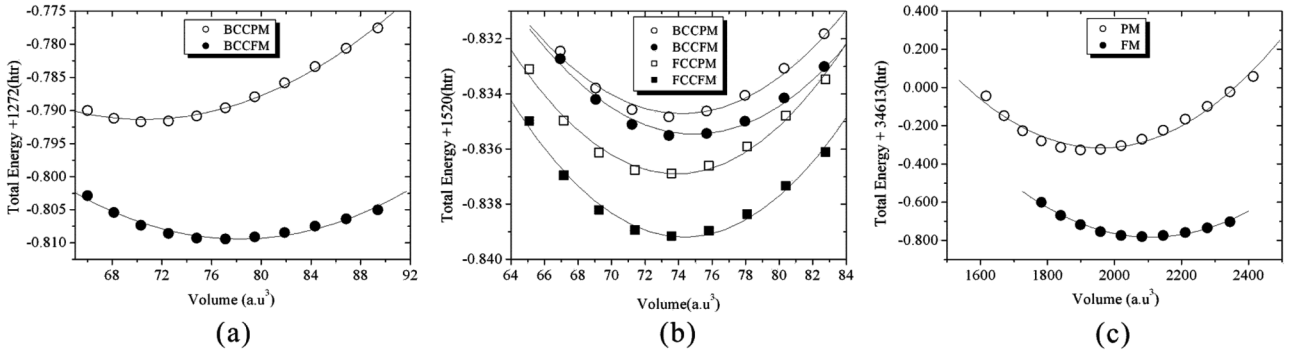

Fig. 1. Total energy as a function of volume for (a) bcc Fe, (b) bcc Ni and fcc Ni, and (c) bcc Ni_1Fe_{26}. Circles (squares) represent bcc (fcc) structures. The filled (open) symbols denote the FM (PM) states.

Table 1. The calculate lattice constant (a) in units of Å and magnetic moment per atom (M) in units of ìB of bcc Fe, bcc Ni, fcc Ni, and bcc Ni_1Fe_{26}. Both the paramagnetic (PM) and ferromagnetic (FM) results are listed. The experimental (Expt.) values for the bcc Fe [13], fcc Ni [13], and bcc Ni_1Fe_{26} [15] and the other theoretical (Other) [12] results are also listed for comparison.

	bcc Fe		bcc Ni		fcc Ni		Ni_1Fe_{26}	
	a (Å)	$M(\mu_B)$	a (Å)	$M(\mu_B)$	a (Å)	$M(\mu_B)$	a (Å)	$M(\mu_B)$
PM	2.76		2.79		3.51		2.76	
FM	2.83	2.17	2.80	0.53	3.52	0.59	2.84	2.24
Expt.	2.87	2.22			3.52	0.61		2.26
Other	2.83, 2.84	2.17	2.80	0.53	3.52	0.62		

Table 2. Calculated angular-momentum decomposed charges and the total magnetic moments M in units of μ_B inside each MT sphere of Ni_1Fe_{26} and bcc Fe. The up (down) arrows represent spin-up (spin-down) states.

	Atom	s (↑/↓)	p (↑/↓)	d (↑/↓)	total (↑/↓)	M (μ_B)
Ni_1Fe_{26}	Ni	0.20/0.22	0.17/0.23	4.56/3.49	4.93/3.94	0.99
	Fe1	0.12/0.12	0.10/0.12	4.07/1.62	4.29/1.86	2.43
	Fe2	0.12/0.12	0.10/0.12	4.00/1.71	4.22/1.95	2.27
	Fe3	0.12/0.12	0.10/0.12	4.00/1.70	4.22/1.94	2.28
bcc Fe	Fe	0.12/0.12	0.10/0.12	3.97/1.72	4.18/1.97	2.21

agreement with the earlier results [15, 17, 19]. The calculated magnetic moment per atom of Ni_1Fe_{26} is 2.24 μ_B, which indicates that the Ni impurity increases the magnetic moment of Fe compared with pure bcc Fe (2.17 μ_B per atom). Furthermore, the enhancement of magnetic moment due to Ni impurity is also consistent with the experimental observations [19].

In order to understand the origin of magnetic moment enhancement due to Ni impurity in bcc Fe, we present the calculated numbers of angular-momentum-decomposed charges and magnetic moments inside each MT sphere of Ni_1Fe_{26} and bcc Fe in Table 2. It can be seen that the magnetic moments within the MT spheres of Ni, Fe1, Fe2, and Fe3 are 0.99, 2.43, 2.27, and 2.28 μ_B, respectively. It is evident from Table 2 that the magnetic moment of Fe1 is much larger than that of bulk bcc Fe. Compared with bcc Fe, the number of spin-up d charges of Fe1 is increased by 0.10, whereas the number of spin-down d charges of Fe1 is decreased by 0.10. This change in occupancy of both spin-up and spin-down d states of Fe1 can be considered as the source of the enhanced ferromagnetic moment.

The calculated orbital-decomposed spin-polarized density of states (DOS) of Ni_1Fe_{26} is presented in Fig. 2 and that of bcc Fe and bcc Ni are also presented for comparison. It is observed that the spin-up states of bcc Fe are partially occupied and the Fermi level (E_F) locates at the spin-down DOS minimum. This feature is typical band structure of bcc metals and separates the lower-lying bonding states from the higher-lying antibonding ones. We found that the DOS of Fe2 and Fe3 are almost similar to that of pure bcc Fe ones. However, the DOS of Fe1 is significantly different near E_F.

When Ni impurity is added to Fe, the potential felt by the valence electrons of Ni is altered due to the neighboring Fe atoms and may not sufficient to keep the valence electrons in truly localized states. Thus, the valence electrons may enter into the higher energy states and they form a virtual bound state (VBS) [20] in the spin-down band just above E_F. It is observed in Fig. 2(d) that the VBS is mainly formed by the unoccupied $e_{g\downarrow}$ band of Ni. Furthermore, since Fe1 atoms locate at the diagonal

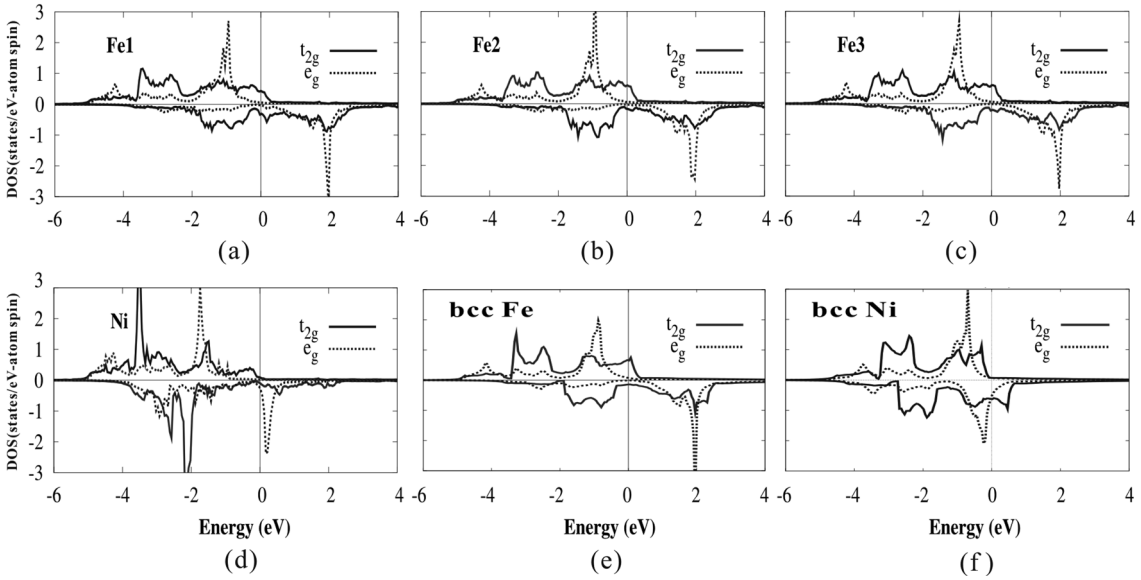

Fig. 2. Atom-projected spin-polarized density of states (DOS) of (a) Fe1, (b) Fe2, (c) Fe3, (d) Ni, (e) bcc Fe, and (f) bcc Ni. The DOS values of spin-down are multiplied by –1, and the Fermi levels (E_F) are set to zero. The solid and dotted lines represent t_{2g} and e_g bands, respectively.

positions of the octahedron cage around the Ni atom, the Fe1 $t_{2g\downarrow}$ wavefunction is able to hybridize with the Ni $e_{g\downarrow}$VBS. This feature was observed at the Fe1 $t_{2g\downarrow}$ band just above E_F as can be seen in Fig. 2(a). Thus, both the spin flip and Fe1 $t_{2g\downarrow}$-Ni $e_{g\downarrow}$ hybridization are considered to be responsible for the enhancement of magnetic moment of Fe. Furthermore, according to our calculations Ni 3*d* band plays a dominant role in bcc Fe particularly near the E_F, but in some cases Ni 3*d* band does not contribute to the transport properties [21].

4. Summary

We investigated the magnetic and electronic properties of Ni_1Fe_{26} in terms of first-principles calculations by using the FLAPW method based on the GGA. The equilibrium lattice constants, magnetic moments, and electronic structures of bcc Fe, bcc Ni, and fcc Ni are also calculated and they are consistent with the previous calculations and experimental observations. The equilibrium lattice constant of Ni_1Fe_{26} was determined in both the PM and FM states. It is shown that Ni impurity slightly increases the bcc Fe lattice constant in the FM state. The calculations also showed that the Ni impurity in bcc Fe favors the enhancement of magnetic moment of Fe. The calculated electronic structures of Ni_1Fe_{26} revealed that the Ni $e_{g\downarrow}$ state is forming the VBS above E_F, which is considered as the origin of the magnetic moment enhancement of the neighboring Fe atom via hybridization between the impurity Ni $e_{g\downarrow}$ and Fe1 $t_{2g\downarrow}$ states.

References

[1] E. A. Owen and Y. H Liu, J. Iron St. Inst. **163**, 132 (1949).
[2] A. R. Williams, V. L. Moruzzi, and C. D. Gelatt, J. Magn. Magn. Mater. **31**, 88 (1983).
[3] R. Meyer and P. Entel, Phys. Rev. B **57**, 5140 (1998).
[4] J. B. Filho and C. A. Kuhnen, Barz. J. Phys. **23**, 288 (1993).
[5] Y. Mishin, M. J. Mehl and D. A. Papaconstantopoulos, Acta Mate. **53**, 4029 (2005).
[6] E. Wimmer, H. Krakauer, M. Weinert, and A. J. Freeman, Phys. Rev. B **24**, 6864 (1981).
[7] M. Weinert, E. Wimmer, and A. J. Freeman, Phys. Rev. B **26**, 4571 (1982).
[8] J. P. Perdew, K. Burke, and M. Ernzerhof, Phys. Rev. Lett. **77**, 3865 (1996).
[9] Y. J. Jin and Jae Il Lee, J. Magnetics **12**(2), 59 (2007).
[10] Y. J. Jin and Jae Il Lee, J. Magnetics **12**(3), 97 (2007).
[11] B. Białek and J. I. Lee, J. Magnetics **12**(3), 93 (2007).
[12] J. H. Lee, T. Shishidou, and A. J. Freeman, Phys. Rev. B **66**, 233102 (2002).
[13] H. J. Monkhorst and J. D. Pack, Phys. Rev. B **13**, 5188 (1976).
[14] F. Birch, Phys. Rev. **71**, 809 (1947).
[15] D.-K. Lee and S. C. Hong, J. Magnetics **12**(2), 68 (2007).
[16] G. Y. Guo and H. H. Wang, Chin. J. Phys. **38**, 949 (2000).
[17] C. Kittel, *Introduction to Solid State Physics 7th ed.* (Wiley, New York, 1996).
[18] L. W. McKeehan, Phys. Rev. **21**, 402 (1923).
[19] J. Crangle and G. C. Hallam, Proc. Roy. Soc. A **272**, 119 (1963).
[20] V. A. Gubanov, A. L. Liechtenstein, and A. V. Postnikov, *Magnetism and the Electronic Structure of Crystals* (Springer, Berlin, 1992).
[21] J. H. Park, S. K. Kwon, and B. I. Min, J. Magnetics **12**(2), 64 (2007).